Indirect nitrous oxide emissions from streams within the US Corn Belt scale with stream order

Peter A. Turner[a,1], Timothy J. Griffis[a], Xuhui Lee[b,c], John M. Baker[a,d], Rodney T. Venterea[a,d], and Jeffrey D. Wood[a]

[a]Department of Soil, Water, and Climate, University of Minnesota, St. Paul, MN 55108; [b]School of Forestry and Environmental Studies, Yale University, New Haven, CT 06511; [c]Yale-Nanjing University of Information, Science and Technology Center on Atmospheric Environment, Nanjing University of Information, Science and Technology, Nanjing, Jiangsu Province 210044, China; and [d]US Department of Agriculture–Agricultural Research Service, St. Paul, MN 55108

Edited by Stephen J. Del Grosso, US Department of Agriculture–Agricultural Research Service, Ft. Collins, CO, and accepted by the Editorial Board June 27, 2015 (received for review February 20, 2015)

N_2O is an important greenhouse gas and the primary stratospheric ozone depleting substance. Its deleterious effects on the environment have prompted appeals to regulate emissions from agriculture, which represents the primary anthropogenic source in the global N_2O budget. Successful implementation of mitigation strategies requires robust bottom-up inventories that are based on emission factors (EFs), simulation models, or a combination of the two. Top-down emission estimates, based on tall-tower and aircraft observations, indicate that bottom-up inventories severely underestimate regional and continental scale N_2O emissions, implying that EFs may be biased low. Here, we measured N_2O emissions from streams within the US Corn Belt using a chamber-based approach and analyzed the data as a function of Strahler stream order (*S*). N_2O fluxes from headwater streams often exceeded 29 nmol N_2O-N $m^{-2}{\cdot}s^{-1}$ and decreased exponentially as a function of *S*. This relation was used to scale up riverine emissions and to assess the differences between bottom-up and top-down emission inventories at the local to regional scale. We found that the Intergovernmental Panel on Climate Change (IPCC) indirect EF for rivers (EF_{5r}) is underestimated up to ninefold in southern Minnesota, which translates to a total tier 1 agricultural underestimation of N_2O emissions by 40%. We show that accounting for zero-order streams as potential N_2O hotspots can more than double the agricultural budget. Applying the same analysis to the US Corn Belt demonstrates that the IPCC EF_{5r} underestimation explains the large differences observed between top-down and bottom-up emission estimates.

aquatic nitrous oxide fluxes | IPCC emission factors | river emission hotspots | regional emission upscaling

N_2O is projected to remain the dominant stratospheric ozone-depleting substance of the 21st century (1) and is a powerful greenhouse gas (GHG) that currently accounts for about 6% of the net radiative forcing associated with long-lived anthropogenic GHGs (2). The detrimental environmental impacts of N_2O have stimulated appeals to regulate emissions from agricultural lands (1, 3), which account for nearly 80% of the global anthropogenic N_2O budget (4, 5). The successful regulation and mitigation of N_2O emissions requires a sound understanding of the direct and indirect emission processes and reduced uncertainty regarding the emission factors (EFs) (6).

The Intergovernmental Panel on Climate Change (IPCC) tier 1 approach uses EFs to provide first-order approximations of annual N_2O emissions based on mechanistic and empirical information that have been constrained by field studies. These EFs are widely used in bottom-up inventories such as the Emission Database for Global Atmospheric Research (EDGAR) (7) and the Global Emissions Initiative (GEIA) (8). These inventories are essential tools for tracking country specific emission trends, assessing thresholds for international treaties, and evaluating the impacts of mitigation policies. Recent independent top-down estimates note large discrepancies with these bottom-up inventories.

Tall-tower and aircraft-based top-down studies use atmospheric concentration data to estimate landscape N_2O fluxes. Several studies using these approaches demonstrate that bottom-up inventories underestimate N_2O emissions by up to ninefold in the Midwest US Corn Belt (9–12), implying that some EFs are too small. An important problem, therefore, is determining which EFs are biased low and how to reduce their uncertainty.

Bottom-up N_2O emission inventories include direct and indirect emission pathways. Direct emissions describe the loss of N_2O produced in soils by microbial processes (e.g., nitrification and denitrification). This source is arguably well constrained as a consequence of more than 1,000 chamber-based emission studies (6, 13). Plant N_2O fluxes, although neglected in direct emissions inventories, appear to be negligible (10). The relatively low direct emission uncertainty range (0.4–3.8 Tg $N{\cdot}y^{-1}$) (14) suggests that this EF (0.003–0.03) (15) is well constrained.

Indirect emissions represent the aggregate of N_2O production from leaching and runoff, human sewage, and atmospheric deposition of reactive nitrogen. Global indirect emission estimates range from 0.23 to 11.9 Tg $N{\cdot}y^{-1}$ (16) and represent nearly two thirds of the uncertainty in the total global N_2O budget (14). In fact, the EF for leaching and runoff (IPCC emission factor: EF_5), which includes emissions from groundwater (EF_{5g}), rivers (EF_{5r}), and estuaries (EF_{5e}), is the single largest source of uncertainty in the bottom-up inventory (14). In the 2006 IPCC Emission Guidelines report, the EF_5 value was reduced from 0.025 to 0.0075 by reducing both the EF_{5g} and EF_{5r} to 0.0025 in response to two studies from New Zealand and the United Kingdom (15). However, recent studies (17–20) suggesting riverine N_2O loss is underestimated by up to threefold notably contradict the EF_{5r} reduction.

Significance

N_2O emissions from riverine systems are poorly constrained, giving rise to highly uncertain indirect emission factors that are used in bottom-up inventories. Using a non–steady-state flow-through chamber system, N_2O fluxes were measured across a stream order gradient within the US Corn Belt. The results show that N_2O emissions scale with the Strahler stream order. This information was used to estimate riverine emissions at the local and regional scales and demonstrates that previous bottom-up inventories based on the Intergovernmental Panel on Climate Change default values have significantly underestimated these indirect emissions.

Author contributions: T.J.G., X.L., and P.A.T. designed research; P.A.T. performed research; T.J.G., X.L., J.M.B., and R.T.V. contributed new reagents/analytic tools; P.A.T. and J.D.W. analyzed data; and P.A.T., T.J.G., and X.L. wrote the paper.

The authors declare no conflict of interest.

This article is a PNAS Direct Submission. S.J.D.G. is a guest editor invited by the Editorial Board.

[1]To whom correspondence should be addressed. Email: turne289@umn.edu.

This article contains supporting information online at www.pnas.org/lookup/suppl/doi:10.1073/pnas.1503598112/-/DCSupplemental.

Uncertainty in the EF_{5r} can be attributed to a scarcity of studies (21, 22), poorly constrained water-air gaseous exchange relationships (23, 24), and high variability in river morphology (25, 26). Further, the EF_{5r} assumes a linear relation between nitrate in water and N_2O emissions (14), the validity of which is the subject of considerable debate (27–30). Finally, N_2O fluxes derived from simple gas exchange models have been shown to underestimate the flux if stream channel hydraulics (i.e., stream flow velocity) are ignored (31), highlighting that stream chemistry alone is not an accurate predictor of N_2O fluxes.

We posit that the indirect N_2O fluxes in agricultural landscapes are highly dependent on stream hierarchy, which is semiquantitatively represented with the Strahler stream order (S), a numerical classification system. Here, we demonstrate that with detailed knowledge of S, N_2O fluxes can be scaled up to the region and help to resolve the discrepancy between top-down and bottom-up N_2O emission estimates in the US Corn Belt.

Results and Discussion

N_2O fluxes in southeastern Minnesota were measured in streams of varying S over a 2-y period. A total of 19 stream systems, representing nine stream orders, were sampled. An exponential function was used to describe the relationship between observed N_2O fluxes (F, nmol N_2O-N·m^{-2}·s^{-1}) and S

$$F = b_0 \exp^{(-b_1 * S)}, \quad [1]$$

where $b_0 = 34 \pm 10.2$ (95% CI) and $b_1 = 0.73 \pm 0.2$, with $R^2 = 0.95$ and 0.58 for binned ($n = 9$) and raw data ($n = 200$), respectively (Fig. 1). Fluxes ranged from below the chamber system detection limit of 0.018 nmol N_2O-N·m^{-2}·s^{-1} (i.e., for the Mississippi River; $S = 9$) to a maximum observed flux of 34.5 nmol N_2O-N·m^{-2}·s^{-1} in a headwater stream ($S = 1$). A Kruskal–Wallis significance test revealed a significant mean rank difference ($P < 0.05$) in fluxes for headwater streams vs. all other stream orders. Further, there was a significant rank difference between fifth- and ninth-order streams, whereas there was no rank difference detected in second- to fifth-order streams. The differences were greatest when testing nonsequential stream orders.

We hypothesize that the exponential decline in N_2O flux is the result of both weakened concentration gradient and lower piston velocities (k) in higher-order streams. Riverine N_2O fluxes are a product of the concentration gradient between the surface water and the overlying atmosphere and a physical gas transfer coefficient (32). We propose two possible mechanisms underlying the emergent pattern shown in Fig. 1 including decreased in situ N_2O production and loading and decreased gas exchange rates.

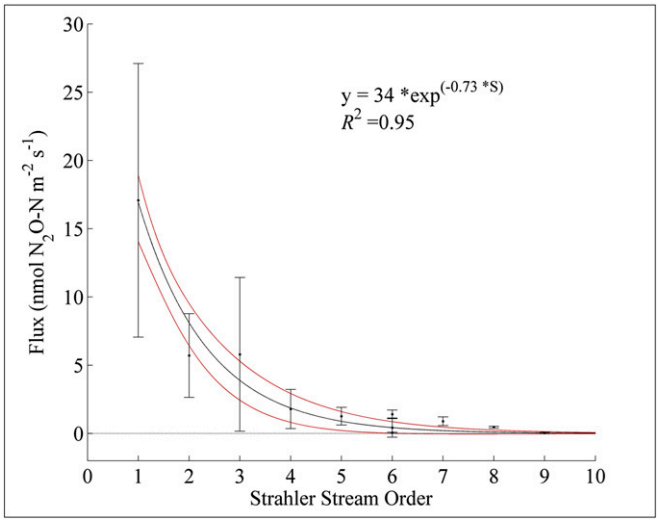

Fig. 1. The relation between N_2O flux and the Strahler stream order in southeastern Minnesota. The black line represents the best fit of an exponential function to the mean flux values measured at each stream order. Red lines represent the 95% CI of the model fit, and error bars indicate 1 SD from the mean.

Mechanism 1. Headwater streams form from surface and subsurface runoff that, in regions with a high density of row crop agriculture, have high nitrate and ammonium loads, and as a consequence, ~45–50% of a watershed's inorganic nitrogen transport can occur in these systems (33, 34). Nitrogen is rapidly transformed via nitrification and removed through denitrification (35) in headwater streams (33), and these processes can quickly produce a surplus of N_2O in the water column. However, the average first-order rate of nitrogen loss within stream channels declines by as much as 90% down the stream order continuum (36). Therefore, production potential declines as stream order increases. Accordingly, we observed a decline in surface water N_2O concentrations from supersaturated (>1,000%) in second-order streams to near equilibrium with atmospheric N_2O in fourth-order streams. Groundwater dissolved gas inputs are an additional N_2O source and are most impactful in low flow headwater systems (37). However, groundwater loading has less of an effect on stream water chemistry with rising stream order (i.e., due to the water volume dilution effect) (37). Collectively, with increasing stream order, N_2O production potential and loading progressively decline, which could account for the pattern shown in Fig. 1.

Mechanism 2. Exchange across the water-atmosphere interface of supersaturated gases is governed by k, which describes the turbulent nature of the stream. An inverse relationship between kCO_2 and S has been observed (38–40), and as a consequence, the highest kCO_2 values are frequently observed in headwater streams (38, 40–42). The same relationship after adjusting for the Schmidt number should be applicable to N_2O, implying that kN_2O increases with declining stream order. Localized areas with high k values (i.e., riffles) have been shown to be strong emission sources (31) if streams are supersaturated (e.g., mechanism 1). However, if the stream is not supersaturated, a high k value alone cannot generate a large flux. Further, a lower k implies a longer total residence time (age) and therefore a greater probability of N_2O reacting with nitrous oxide reductase (*nos*), the enzyme that catalyzes the final step in the denitrification reaction sequence: the reduction of N_2O to N_2 (43). Although this has not been documented in river systems, this potential mechanism merits further research to determine its importance and its ability to weaken the water-atmosphere N_2O concentration gradient. We posit that these two mechanisms, individually or combined, account for the relationship observed in Fig. 1 and require further study to elucidate their relative importance.

In our study, the variability of N_2O flux (i.e., the SD) scaled with stream order, leading to a tightly constrained relation for high order systems (Fig. 1). These observations imply a robust constraint on high-order (fifth-order and higher) emissions and that this pattern could be applied to similar systems (44). Conversely, much larger uncertainty in low-ordered systems (45, 46) exists, indicating that caution must be taken before generalizing our scaling function outside of the US Corn Belt. Headwater streams displayed the greatest uncertainty and their high variability has also been noted in CO_2 evasion work (41). Low-order streams receive tile drainage outflow and groundwater from springs giving rise to localized "hotspots" of N_2O loss (45), similar to those seen in methane evasion work (41).

To test the appropriateness of the default IPCC EF_{5r} value, we used Eq. 1 to up-scale emissions within the observed concentration footprint (50-km radius) of our tall-tower N_2O flux station (9). Land use in this study area consists of 70% crops and pasture, 14%

mixed vegetation, 11% forest, 3% developed, and 2% open water and is representative of the US Corn Belt. Streams in the area represent only a small fraction (0.16%) of the total surface area. Using default IPCC EFs for direct and indirect emissions, we provide a conservative estimate of the local agricultural N_2O budget in addition to our up-scaled riverine emissions.

Whole-river emissions are the product of our scaling function and river area over a predicted ice-free period. We estimated the annual riverine N_2O loss by coupling Eq. 1 with detailed geospatial datasets on stream length and width. Headwater streams ($S = 1$) were the strongest sources, emitting 60% of the riverine budget. The remaining streams in the study area (S = 2–5) contributed 14%, 8%, 10%, and 8% to the up-scaled riverine emission budget, respectively. This disproportionate flux distribution was a result of a threefold greater mean flux density from headwater streams (17.1 nmol N_2O-N·m^{-2}·s^{-1}) than second-order streams (5.7 nmol N_2O-N·m^{-2}·s^{-1}).

Using the IPCC tier 1 methodology (15), the total agricultural (direct + indirect) N_2O emissions from the tall-tower footprint were 0.2 Gg N_2O-N·y^{-1}, which corresponds to a flux density of 0.25 (0.08–0.6) nmol N_2O-N·m^{-2}·s^{-1}. Indirect and direct sources contributed 22% and 78%, respectively, to the tier 1 budget. Here, the default EF_{5r} predicts that rivers emitted 0.01 Gg N_2O-N·y^{-1}, which represents just over 5% of the total N_2O-N emissions. Our scaling method predicted a riverine source of 0.09 (0.04–0.18) Gg N_2O-N·y^{-1} (Fig. 2*A*), an estimate that is nine times greater than the source predicted by the default EF_{5r}, signaling a significant bottom-up bias in the EF_{5r}. Replacing the EF_{5r} with our scaling function suggests that the total tier 1 bottom-up agricultural emissions have been underestimated by 40%. Accounting for this potential bias increases the predicted bottom-up flux density within the tall-tower source footprint to 0.36 nmol N_2O-N·m^{-2}·s^{-1} (Fig. 2*C*). This estimate is in excellent agreement with the top-down tall-tower measured ensemble flux of 0.35 (0.3–0.4) nmol N_2O-N·m^{-2}·s^{-1} (9), indicating that top-down and bottom-up budgets can be reconciled by applying our stream order scaling function. Our study suggests that an appropriate EF_{5r} for the tall-tower source footprint should be closer to 2%, assuming the average application rate of nitrogen fertilizer (88.8 kg N·ha^{-1}) (47), which is in agreement with a recent independent investigation (18).

Based on the tier 1 methodology, we estimated the agricultural N_2O budget of the US Corn Belt at 58 (15–256) Gg N_2O-N·y^{-1}, of which 6% or 3.5 Gg N_2O-N·y^{-1} emanates from rivers (Fig. 2*B*). In this region, watersheds with high agricultural land use (>40%) occupy 93 million ha (58 million ha under active row-crop cultivation). Applying Eq. 1 to these watersheds and using river area data, we obtained a riverine emission of 19.5 (9.3–41.2) Gg N_2O-N·y^{-1}. Our findings suggest that riverine N_2O emissions are underestimated by at least 16 Gg N_2O-N·y^{-1} for the Corn Belt and on average by 29 kg N_2O-N·km^{-2}·y^{-1} in watersheds whose cropland fractions are greater than 40% (Fig. 3). Including this source results in a 27% increase in the total tier 1 emission estimate from 58 to 75 Gg N_2O-N·y^{-1} (Fig. 2*B*). These findings indicate that a more appropriate regional EF_{5r} is closer to 1.5% (0.7–3%) if the average nitrogen inputs, agricultural coverage (48), and runoff scaling factor (15) are used.

It is important to note that our revised EF_{5r} may not be applicable to areas that are nitrogen limited. Our conservative land use threshold of >40% cropland was chosen because the

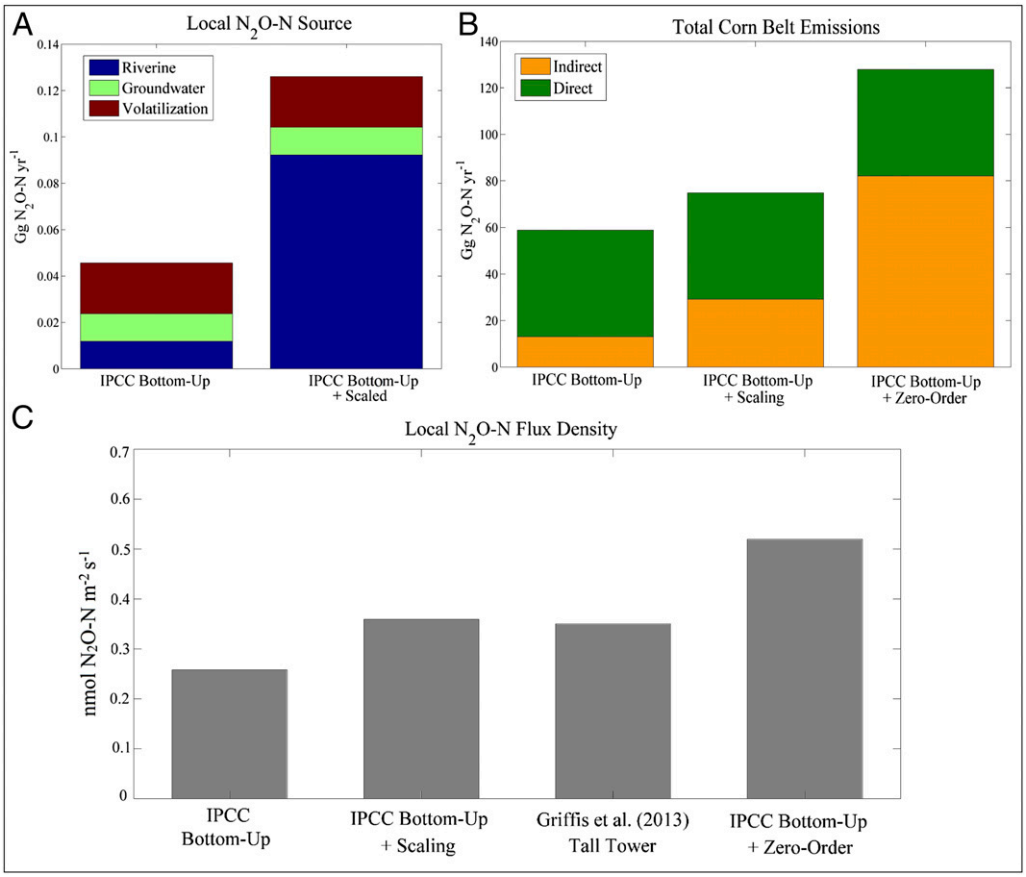

Fig. 2. Results from upscaling N_2O emissions. (*A*) A comparison of local indirect N_2O-N sources from default IPCC EFs and our scaling method. (*B*) Total US Corn Belt emissions from the three methods. (*C*) The flux densities from the tall-tower source footprint for each method.

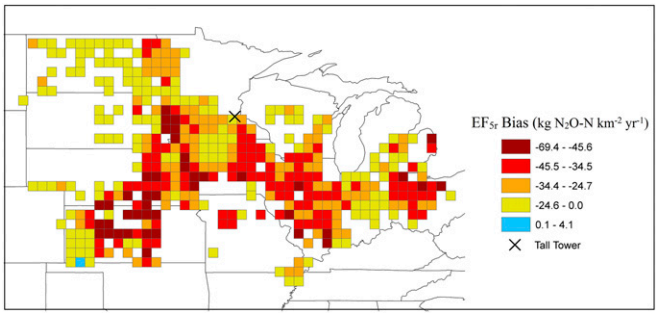

Fig. 3. The first-order default EF_{5r} underestimation from the Corn Belt region. The bias is defined as the difference between IPCC EF_{5r} emissions and the results from stream order scaling.

corn and soybean systems prevalent in the US Corn Belt indirectly identify areas of high nitrogen loading. Although average nitrogen application rates vary, from 1994 to 2001, the average applied to all arable lands within the US Corn Belt was 48 kg $N{\cdot}ha^{-1}$ (49). As such, we propose that agriculturally dominated watersheds receiving rates greater than 48 kg $N{\cdot}ha^{-1}$ will be subject to similar indirect emissions and emission factors as observed in this study. We believe that the majority of the annual riverine N_2O budget will originate from those watersheds and that their total area globally exceeds 235 million ha. Following the United States (93 million ha), the largest regions meeting these criteria are China (69 million ha), Europe (43 million ha), and India (30 million ha). The remaining watersheds are likely to be small N_2O sources, and the default 2006 IPCC EF_{5r} value should be appropriate for these cases (50).

The application of our methodology to the global scale is limited by two main factors. First, the scaling relation described in Fig. 1 is likely applicable to watersheds that are dominated by cropland systems with nitrogen inputs greater than 48 kg $N{\cdot}ha^{-1}$. Second, our stream order width was estimated using methodologies limited to the contiguous United States and Africa (51). At this time, we are unaware of an existing accurate global river width dataset, and this represents an important limitation for application of our method to other regions. We believe this is an important research need, especially in countries with significant agricultural production including corn (e.g., China, India, Brazil, and others).

The above analyses did not consider the role of fine-scale drainage features. Zero-order streams, or microflow stream channels, extend upland of headwater streams, are highly episodic, and are likely hot spots of nitrogen processing (52). Zero-order stream systems form at the intersection of terrestrial and aquatic environments. However, because of their episodic nature and low spatial coverage, N_2O flux observations are severely lacking. Advancements in Light Detection and Ranging (LiDAR) remote sensing have made it possible to identify episodic microflow paths that may activate following snowmelt and precipitation events. The microflow paths are produced from high resolution (1 m) elevation maps that predict surface water movement. From these data, zero-order streams represent the most common stream order. We estimate that their length is 33 times that of first-order streams in the tall-tower footprint. By extrapolating Eq. 1 to include zero-order streams, we suggest that they exert a significant influence on the N_2O budget by increasing the local emissions to 0.41 Gg N_2O-$N{\cdot}y^{-1}$ in the tall-tower footprint, or 101% greater than the default IPCC estimate. Scaling zero-order streams to the Corn Belt increases indirect emissions to 82 Gg N_2O-$N{\cdot}y^{-1}$, whereas the total emissions double to 129 Gg N_2O-$N{\cdot}y^{-1}$. However, the uncertainty in N_2O emissions related to zero-order streams is large because we lack direct observational data, the reactivation timing is uncertain, and the microscale watershed threshold necessary to form a zero-order stream is highly variable. Regardless, there appears to be growing evidence of their importance in closing the gap between bottom-up and top-down emission estimates for the US Corn Belt.

Materials and Methods

N_2O Flux Sampling. N_2O fluxes were measured in the field using a flow-through non–steady-state chamber system adapted for deployment in rivers. The floating chamber consisted of an aluminum lid with a pressure equilibration vent buoyed by foam insulation and covered with reflective material. The chamber enclosed a surface area of 0.145 m^2 with a headspace volume of ~0.0147 m^3.

Headspace gas was pulled through a Teledyne gas filter correlation N_2O analyzer (Model M320EU2; Teledyne Instruments), and the dry mole fraction was recorded at a sampling frequency of 1 Hz using a data-logger (model 23X; Campbell Scientific). The analyzer was powered in the field by deep cycle 12 V batteries wired in parallel to a DC-to-AC inverter. The chamber system has a minimum detectable flux of 0.028 nmol $N_2O{\cdot}m^{-2}{\cdot}s^{-1}$ (53). The analyzer was calibrated at the beginning of the season using an analytical grade standard and zeroed two times per month using N_2 gas. The concentration precision of the analyzer was 1.5 $nmol{\cdot}mol^{-1}$, and the flux measurement precision was 0.003 $nmol{\cdot}m^{-2}{\cdot}s^{-1}$ (53).

The raw data were processed in Matlab (Matlab, Version R2012a; Mathworks). Fluxes were calculated according to

$$F = \frac{\rho V \Delta}{A}, \quad [2]$$

where ρ ($mol{\cdot}m^{-3}$) is the molar density of dry air, A (m^2) is the surface area enclosed by the chamber, V (m^3) is the chamber volume, and Δ (nmol $N_2O{\cdot}mol^{-1}{\cdot}s^{-1}$) is the rate of change of N_2O concentration in the chamber headspace determined from linear regression (53). Before calculating the chamber N_2O fluxes, a wavelet denoising technique was applied to the raw concentration data. This technique reduced the effect of instrument noise and improved the signal to noise ratio (53). We eliminated all chamber flux data when the linear regression R^2 value was less than 0.9.

Upscaling. Nonlinear regression analysis was performed using the "fitnlm" function in Matlab. Local stream order data were downloaded from the Minnesota Department of Natural Resources. Mean North American stream order width (51) was used to generate stream area. Stream order areal estimates were applied to our nonlinear function to predict river emissions over a 214-d period (Day of Year 91–305).

The extent of the Corn Belt is subjective and lacks boundaries. Our definition was determined by selecting HUC12 subwatersheds with greater than 40% agriculture from 13 states in the Midwest (North Dakota, South Dakota, Nebraska, Kansas, Minnesota, Iowa, Missouri, Arkansas, Wisconsin, Illinois, Ohio, Indiana, and Michigan). Regional stream order data (NHDPlus, V.2; Horizon Systems Corp.) were used in our nonlinear model. The regional dataset is at a lower resolution than the local stream order and as a consequence underestimated stream length. A comparison of Minnesota streams determined a scaling factor (1.4) was appropriate to apply to the regional data to correct for this underestimation.

Default tier 1 IPCC methodologies were used to estimate N_2O emissions (15). This budget included direct emissions from soils from synthetic and organic nitrogen application, indirect emissions from the volatilization of synthetic and organic fertilizer, rivers, and groundwater. We did not account for emissions from natural systems, industry, grazing livestock, organic soils, crop residues, and legumes. Annual rates of synthetic and organic fertilizer application were used.

Zero-order streams were estimated from LiDAR data provided by the Minnesota Geospatial Information Office that was processed using ArcMap. A threshold of 250 m^2 was set before a stream would "activate." We assumed a period of 2 mo of active emissions that would include spring thaw and periodic precipitation events. Zero-order width was estimated using a regression equation from North American stream width data (51).

ACKNOWLEDGMENTS. We thank Joel Fassbinder, Matt Erickson, Mike Dolan, William Breiter, Kendall King, and Natalie Schultz for field and laboratory assistance. This work was supported by US Department of Agriculture (USDA) Grant USDA-NIFA 2013-67019-21364 (to T.J.G. and X.L.), the USDA-Agricultural Research Service, National Oceanic and Atmospheric Administration Grant NA13OAR4310086, the Minnesota Supercomputing Institute for Advanced Computational Research (https://www.msi.umn.edu/), and X.L. also acknowledges support by the Ministry of Education of China (Grant PCSIRT).

1. Ravishankara AR, Daniel JS, Portmann RW (2009) Nitrous oxide (N2O): The dominant ozone-depleting substance emitted in the 21st century. *Science* 326(5949):123–125.
2. Hartmann DL, et al. (2013) Observations: Atmosphere and surface. *Climate Change 2013: The Physical Science Basis*, Intergovernmental Panel on Climate Change (Cambridge Univ Press, New York), pp 159–254.
3. Kanter D, et al. (2013) A post-Kyoto partner: Considering the stratospheric ozone regime as a tool to manage nitrous oxide. *Proc Natl Acad Sci USA* 110(12):4451–4457.
4. Davidson EA (2009) The contribution of manure and fertilizer nitrogen to atmospheric nitrous oxide since 1860. *Nat Geosci* 2(9):659–662.
5. Crutzen PJ, Mosier AR, Smith KA, Winiwarter W (2008) N2O release from agro-biofuel production negates global warming reduction by replacing fossil fuels. *Atmos Chem Phys* 8(2):389–395.
6. Shcherbak I, Millar N, Robertson GP (2014) Global metaanalysis of the nonlinear response of soil nitrous oxide (N2O) emissions to fertilizer nitrogen. *Proc Natl Acad Sci USA* 111(25):9199–9204.
7. European Commission Joint Research Centre/Netherlands Environmental Assessment Agency (2011) Emissions database for Global Atmospheric Research, v.4.2. Available at edgar.jrc.ec.europa.eu. Accessed July 8, 2015.
8. IGAC/iLEAPS/AIMES (2014) Global Emissions Initiative (GEIA). Available at www.geiacenter.org. Accessed July 8, 2015.
9. Griffis TJ, et al. (2013) Reconciling the differences between top-down and bottom-up estimates of nitrous oxide emissions for the U.S. Corn Belt. *Global Biogeochem Cycles* 27(3):746–754.
10. Zhang X, et al. (2014) Quantifying nitrous oxide fluxes on multiple spatial scales in the Upper Midwest, USA. *Int J Biometeorol* 59(3):299–310.
11. Kort EA, et al. (2008) Emissions of CH4 and N2O over the United States and Canada based on a receptor-oriented modeling framework and COBRA-NA atmospheric observations. *Geophys Res Lett* 35(18):1–5.
12. Miller SM, et al. (2012) Regional sources of nitrous oxide over the United States: Seasonal variation and spatial distribution. *J Geophys Res Atmos* 117(D6):1–13.
13. Stehfest E, Bouwman L (2006) N2O and NO emission from agricultural fields and soils under natural vegetation: Summarizing available measurement data and modeling of global annual emissions. *Nutr Cycl Agroecosyst* 74(3):207–228.
14. Nevison C (2000) Review of the IPCC methodology for estimating nitrous oxide emissions associated with agricultural leaching and runoff. *Chemosphere, Glob Chang Sci* 2(3-4):493–500.
15. De Klein C, et al. (2006) N2O emissions from managed soils, and CO2 emissions from lime and urea application. *IPCC Guidelines for National Greenhouse Gas Inventories, Prepared by the National Greenhouse Gas Inventories Programme, 4* (Institute for Global Environmental Strategies, Hayama, Japan), Vol 4, pp 1–54.
16. Mosier A, Kroeze C, Nevison C, Oenema O, Seitzinger S (1998) Closing the global N2O budget: nitrous oxide emissions through the agricultural nitrogen cycle. *Nutr Cycl Agroecosyst* 52(2-3):225–248.
17. Yu Z, et al. (2013) Nitrous oxide emissions in the Shanghai river network: Implications for the effects of urban sewage and IPCC methodology. *Glob Change Biol* 19(10):2999–3010.
18. Outram FN, Hiscock KM (2012) Indirect nitrous oxide emissions from surface water bodies in a lowland arable catchment: A significant contribution to agricultural greenhouse gas budgets? *Environ Sci Technol* 46(15):8156–8163.
19. Hinshaw SE, Dahlgren RA (2013) Dissolved nitrous oxide concentrations and fluxes from the eutrophic San Joaquin River, California. *Environ Sci Technol* 47(3):1313–1322.
20. Beaulieu JJ, et al. (2011) Nitrous oxide emission from denitrification in stream and river networks. *Proc Natl Acad Sci USA* 108(1):214–219.
21. Clough TJ, Bertram JE, Sherlock RR, Leonard RL, Nowicki BL (2006) Comparison of measured and EF5-r-derived N2O fluxes from a spring-fed river. *Glob Change Biol* 12(2):352–363.
22. Clough TJ, Buckthought LE, Kelliher FM, Sherlock RR (2007) Diurnal fluctuations of dissolved nitrous oxide (N2O) concentrations and estimates of N2O emissions from a spring-fed river: Implications for IPCC methodology. *Glob Change Biol* 13(5):1016–1027.
23. Cole JJ, Caraco NF (1998) Atmospheric exchange of carbon dioxide in a low-wind oligotrophic lake measured by the addition of SF6. *Limnol Oceanogr* 43(4):647–656.
24. Beaulieu JJ, Shuster WD, Rebholz JA (2012) Controls on gas transfer velocities in a large river. *J Geophys Res Biogeosci* 117(G2):1–13.
25. Beaulieu JJ, Arango CP, Hamilton SK, Tank JL (2008) The production and emission of nitrous oxide from headwater streams in the Midwestern United States. *Glob Change Biol* 14(4):878–894.
26. Wang S, et al. (2009) The spatial distribution and emission of nitrous oxide (N2O) in a large eutrophic lake in eastern China: Anthropogenic effects. *Sci Total Environ* 407(10):3330–3337.
27. Rosamond MS, Thuss SJ, Schiff SL, Elgood RJ (2011) Coupled cycles of dissolved oxygen and nitrous oxide in rivers along a trophic gradient in southern Ontario, Canada. *J Environ Qual* 40(1):256–270.
28. Rosamond MS, Thuss SJ, Schiff SL (2012) Dependence of riverine nitrous oxide emissions on dissolved oxygen levels. *Nat Geosci* 5(10):715–718.
29. Xia Y, et al. (2013) Is indirect N2O emission a significant contributor to the agricultural greenhouse gas budget? A case study of a rice paddy-dominated agricultural watershed in eastern China. *Atmos Environ* 77(2013):943–950.
30. Venkiteswaran JJ, Rosamond MS, Schiff SL (2014) Nonlinear response of riverine N2O fluxes to oxygen and temperature. *Environ Sci Technol* 48(3):1566–1573.
31. Reay DS, Smith KA, Edwards AC (2003) Nitrous oxide emission from agricultural drainage waters. *Glob Change Biol* 9(3):195–203.
32. Raymond PA, Cole JJ (2001) Gas exchange in rivers and estuaries: Choosing a gas transfer velocity. *Estuaries* 24(2):312.
33. Peterson BJ, et al. (2001) Control of nitrogen export from watersheds by headwater streams. *Science* 292(5514):86–90.
34. Alexander RB, Boyer EW, Smith RA, Schwarz GE, Moore RB (2007) The role of headwater streams in downstream water quality. *J Am Water Resour Assoc* 43(1):41–59.
35. Mulholland PJ, et al. (2008) Stream denitrification across biomes and its response to anthropogenic nitrate loading. *Nature* 452(7184):202–205.
36. Alexander RB, Smith RA, Schwarz GE (2000) On the delivery of nitrogen to the Gulf of Mexico. *Nature* 403(February):758–761.
37. Jones JB, Mulholland PJ (1998) Influence of drainage basin topography and elevation on carbon dioxide and methane supersaturation of stream water. *Biogeochemistry* 40(1):57–72.
38. Butman D, Raymond PA (2011) Significant efflux of carbon dioxide from streams and rivers in the United States. *Nat Geosci* 4(12):839–842.
39. Raymond PA, et al. (2012) Scaling the gas transfer velocity and hydraulic geometry in streams and small rivers. *Limnol Oceanogr Fluids Environ* 2(1):41–53.
40. Raymond PA, et al. (2013) Global carbon dioxide emissions from inland waters. *Nature* 503(7476):355–359.
41. Crawford JT, Striegl RG, Wickland KP, Dornblaser MM, Stanley EH (2013) Emissions of carbon dioxide and methane from a headwater stream network of interior Alaska. *J Geophys Res Biogeosci* 118(2):482–494.
42. Wallin MB, et al. (2011) Spatiotemporal variability of the gas transfer coefficient (KCO2) in boreal streams: Implications for large scale estimates of CO 2 evasion. *Global Biogeochem Cycles* 25(3):1–14.
43. Maier RM, Pepper IL, Gerba CP (2009) *Environmental Microbiology* (Elsevier, Burlington, MA), 2nd Ed.
44. Beaulieu JJ, Shuster WD, Rebholz JA (2010) Nitrous oxide emissions from a large, impounded river: The Ohio River. *Environ Sci Technol* 44(19):7527–7533.
45. Hasegawa K, Hanaki K, Matsuo T, Hidaka S (2000) Nitrous oxide from the agricultural water system contaminated with high nitrogen. *Chemosphere Glob Chang Sci* 2(3-4):335–345.
46. Harrison J (2003) Patterns and controls of nitrous oxide emissions from waters draining a subtropical agricultural valley. *Global Biogeochem Cycles* 17(3):1–13.
47. Potter P, Ramankutty N, Bennett EM, Donner SD (2011) *Global Fertilizer and Manure, Version 1: Nitrogen Fertilizer Application* (NASA Socioeconomic Data and Applications Center, Palisades, NY).
48. Fry J, et al. (2011) Completion of the 2006 National Land Cover Database for the Conterminous United States, *Photogrammetric Engineering and Remote Sensing* 77(9):858–864.
49. Potter P, Ramankutty N, Bennett EM, Donner SD (2011) Global Fertilizer and Manure, Version 1: Nitrogen Fertilizer Application (NASA Socioeconomic Data and Applications Center (SEDAC), Palisades, NY). Available at dx.doi.org/10.7927/H4Q81B0R. Accessed August 29, 2014.
50. Dong LF, Nedwell DB, Colbeck I, Finch J (2004) Nitrous oxide emissions from some English and Welsh rivers and estuaries. *Water Air Soil Pollut* 4:127–134.
51. Downing JA, et al. (2012) Global abundance and size distribution of streams and rivers. *Inl Waters* 2(4):229–236.
52. McClain ME, et al. (2003) Biogeochemical hot spots and hot moments at the interface of terrestrial and aquatic ecosystems. *Ecosystems (N Y)* 6(4):301–312.
53. Fassbinder JJ, Schultz NM, Baker JM, Griffis TJ (2013) Automated, low-power chamber system for measuring nitrous oxide emissions. *J Environ Qual* 42(2):606–614.

Supporting Information

Turner et al. 10.1073/pnas.1503598112

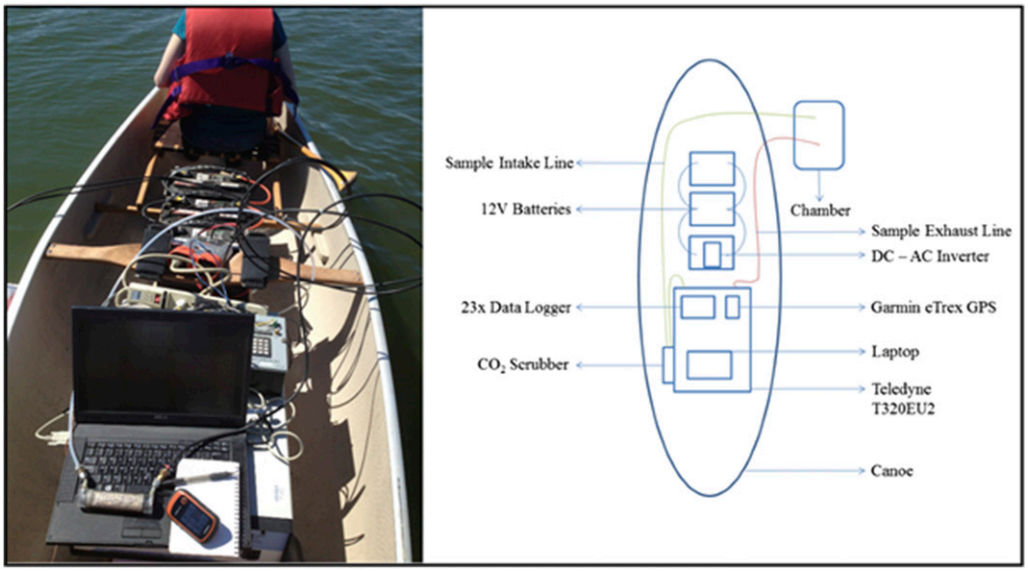

Fig. S1. Photograph and diagram of the system used in this study to sample N_2O flux.